Active disturbance rejection control of a strongly nonlinear and disturbed piezoelectric actuator devoted to robotic hand

Sofiane KHADRAOUI [1], Micky RAKOTONDRABE[2,*], *Member, IEEE,* and Gerardo FLORES[3]

***Abstract*— The target of this paper is to model and to design a controller for a piezoelectric actuator that is devoted to robotic hand. The actuator is characterized by the following properties simultaneously: strong asymmetrical hysteresis nonlinearity, creep nonlinearity, and oscillations in its dynamics. Moreover, the actuator is also exhibited to external disturbance which is the manipulation force. To account for these specificities, we propose to use the generalized Bouc-Wen model for the hysteresis, along with a lumped disturbance term that encompasses the creep and the external force. We also propose to use a high order model for the dynamics. Then, an active disturbance rejection in combination with an extended state observer is suggested and designed as control law. Experiments are carried out and demonstrate the efficiency of the proposed approach.**

I. INTRODUCTION

Piezoelectric actuators are widely used in devices that require precise and high dynamic positioning. Examples include: hard disk drive [1], medical microrobots [2], dental machines [3], diesel engine injectors [4], scanning probe microscopes [5], or robotic hands [6]. This recognition is principally thanks to the high resolution they can offer (down to nanometers), the high bandwidth they can perform (up to tens of kiloHertz), the high force density some of them can provide (up to 1kN for small piezostacks), and the fact that they are powered electrically making them easily integrated. Within the French ECOSYSPRO project, we develop a robotic hand that is capable to pick fragile objects (high end pieces of pottery) and to maintain them during automatized carving and/or painting tasks. Piezoelectric actuators have been chosen to actuate the robotic hand because the precision of the carving/painting should be better than $5\mu m$ to ensure high end art object. Moreover, such actuators will be able to quickly reject the disturbances caused by the carving tasks onto the object and thus to ensure the art quality (drawing, machining...). Finally, if needed, advanced design methods and approaches available in the literature for piezoelectric actuators available can still be applied when designing the robotic hand [7]–[9]. For stability concern, the robotic hand is based on three piezoelectric actuators spaced of 120^o as displayed in Fig 1-a. The hand itself is used as the terminal organ (or end-effector) of a parallel Delta-robot for large and coarse distance pick and place.

[1]: the Department of Electrical Engineering, University of Sharjah, Sharjah, United Arab Emirates. email: sofiane.khadraoui@gmail.com
[2]: Laboratoire Génie de Production, National School of Engineering in Tarbes (ENIT-INPT), University of Toulouse, email: mrakoton@enit.fr
[3]: Centro de Investigaciones en Optica, Leon Mexico, email: gflores@cio.mx
[*]: corresponding author.

Despite the above cited advantages of piezoelectric actuators, they also have drawbacks. First, they exhibit strong nonlinearities that will degrade the overall performances if ignored: the creep phenomenon and the hysteresis. Second, most of the structures of these actuators - mainly bending cantilevers and stack structures - are typified by badly damped vibrations which affect the overall stability of the tasks if not properly controlled. For the concerned robotic hand, these negative properties will definitely degrade the quality of the objects carving and painting whilst their breakages could even occur in the worst situation. Consequently the control of the actuators are mandatory. Control of piezoelectric actuators have raised numerous studies in the literature. They can be categorized into feedforward and feedback architectures as briefly described below.

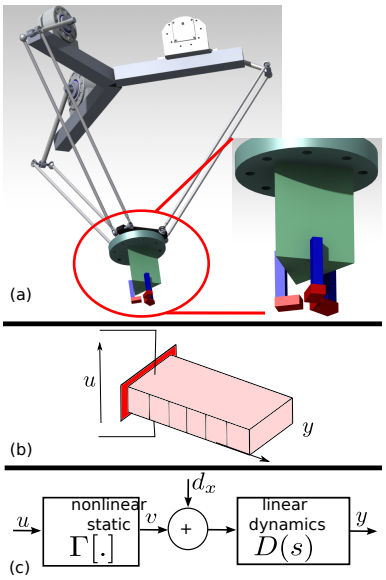

Fig. 1: (a): parallel robotic platform. (b): robotic hand with three piezoelectric actuated fingers. (c): Hammerstein apporximation of a piezoelectric actuator.

Feedforward control architecture has been applied for the creep [10], for the hysteresis [11], [12] and for the vibrations [13], [14] independently. In [15], [16], all of the three phenomena were controlled simultaneously by putting the individual controllers in cascade. The advantages of feedforward are the low cost and the high integration since no external sensor is used. In counterpart, its principal limit is the lack of robustness against models uncertainties and against external disturbance. Due to this, feedforward control

architecture is not suitable to the studied robotic hand because the manipulated object itself acts as perturbation when interacting with the actuators, additionally to the carving task which also disturbs. In feedback control architecture, numerous approaches have been used including: PID structure with experimental or analytical tuning [17], position positive feedback approach [18], adaptive approach [19], robust approach such as H_∞ and interval techniques [20]–[22], and Lyapunov based approach such as sliding mode and backstepping techniques [23]. These previous works permitted to reach the desired performances whilst guaranteeing a certain robustness. Overall, synthesizing feedback control becomes very challenging when the above mentioned properties (nonlinearities, badly damped vibrations) become very strong. The challenge increases if these properties occur simultaneously from the same system.

In this paper, we consider the feedback control of the piezoelectric actuators of the robotic hand by taking into account the following properties simultaneously:
- the creep nonlinearity which will be considered as internal disturbance,
- the hysteresis nonlinearity which will be taken as strongly asymmetric,
- the badly damped vibrations which will be lumped in the dynamic model of the actuator,
- external disturbances which encompass the interaction force between the actuator and the manipulated object.

The contribution of this work versus the literature is the fact we we account for all these properties together. Moreover, we will assume the hysteresis to be strongly asymmetrical, contrary to that used in the previous works. This assumption is motivated by the fact that the weight of the manipulated object makes the piezoelectric actuators work and behave asymmetrically for back and for forth movements. Moreover, the hysteresis asymmetry is also due to imperfection of fabrication and mechanical asymmetry in the system (actuator + mechanical support and amplifier). To reach the target, we propose to approximate the hysteresis with the generalized Bouc-Wen model, to rassemble the creep and the manipulation force in a intermediary disturbance and to account for the badly damped vibrations in a high order dynamic representation. The overall model has therefore a Hammerstein architecture combined with the intermediary disturbance. Then, a nonlinear active distrubance rejection control (ADRC) technique is suggested and adapted to design a robust controller for the actuators. Simulation and experiments are carried out which demonstrate the efficiency of the controller.

The paper is organized as follows. In section-II, we present the robotic hand and the actuator as well as the model. The ADRC controller design is presented in section-III. Section-IV presents the simulation and experimental results respectively. Finally, conclusions and perspectives are given in Section-V.

II. Presentation of the system and modeling

A. The robotic hand and its actuators

The three piezoelectric actuators based robotic hand serves as the end-effector of a parallel robot, see . Each actuator of the hand is a piezostack (Fig 1-b) with rectangular section of $5mm \times 10mm$ allowing it to provide force up to $2kN$ which are sufficient to manipulate and hold ceramics pottery. The length of the piezostack is $30mm$. A screw based adjustment block on the top of the robotic hand allows to open or close simultaneously the three actuators and thus to adjust the initial gap before actuation. Because the three piezoelectric actuators are similar and are subjected to the same constrains, we only study the modeling and control of one of them.

B. Modeling the piezoelectric actuator

The generalized Bouc-Wen (GBW) model is one of the models capable to approximate an asymmetrical hysteresis phenomenon. Like the classical Bouc-Wen model (CBW), the GBW has an interesting structure allowing to do analysis and synthesis much easier than the other hysteresis models (Preisach, Prandtl-Ishlinskii). In [24], we used the GBW to model the piezoelectric actuator of the robotic hand studied in this paper. A first-order dynamics was added to this to track the dynamics by assuming that the actuator did not exhibit badly damped vibrations. In this paper, we propose to consider these vibrations by considering a n^{th} order dynamics. Moreover, we account for the creep nonlinearity and the interaction force with the manipulated object by lumping them in a disturbance. Hence, we propose the model:

$$y^{(n)} + a_{n-1}y^{(n-1)} + \cdots + a_1\dot{y} + y = a_0(v + d_x) \qquad (1)$$

where: $y[\mu m]$ is the displacement from the actuator, $d_x = d_{creep} + F_m$ is the disturbance composed of the creep phenomenon d_{creep} (internal disturbance) and the interaction force F_m (external disturbance), and v is an intermediary input which is described by Eq 2 to account for hysteresis phenomenon:

$$\begin{cases} v = du - h \\ \\ \dot{h} = \dot{u}\left(\alpha - |h|^m \phi(u, \dot{u}, h)\right) \end{cases} \qquad (2)$$

where $u[V]$ is the driving voltage and h is an internal hysteresis state. Second row of Eq 2 corresponds to the state equation. The set Eq 2 corresponds to the Bouc-Wen class of models. Term $\phi(u, \dot{u}, h)$ depends on the model itself.

In the model Eq 1-Eq 2, coefficients a_i $(i = 1 \rightarrow n-1)$ are the dynamic part parameters, d indicates an average slope of the gain in the (u, y)-map, and α and m indicate the strength of the hysteresis. $\phi(u, \dot{u}, h)$ will be a specific nonlinear function related to the GBW model for our case. Meanwhile, another advantage of the proposed controller design in this paper is that we do not need to explicit $\phi(u, \dot{u}, h)$. Fig 1-c is a schematic diagram of the model Eq 1-Eq 2 which shows that it has a Hammerstein structure augmented with an intermediary disturbance. In the figure, the dynamics of

the left-side of Eq 1 is represented by the transfer function $D(s)$.

III. ADRC CONTROLLER DESIGN

Integrating both sides of second equation of the GBW model in Eq 2 results in:

$$h = g(u) = \int \dot{u}\left(\alpha - |h|^{m}\,\phi(u,\dot{u},h)\right) \tag{3}$$

Thus, $v = du - g(u)$. Substituting v into the dynamic part in Eq 1 leads to:

$$y^{(n)} + a_{n-1}y^{(n-1)} + \cdots + a_1\dot{y} + a_0 y = bu - a_0 g(u) + a_0 d_x \tag{4}$$

where $b = a_0 d$. Eq 4 can be rewritten as

$$y^{(n)} = -a_{n-1}y^{(n-1)} - \cdots - a_1\dot{y} - a_0 y + bu - a_0 g(u) + a_0 d_x \tag{5}$$

Let $f(t, y^{(n-1)}, \cdots, y, u, \dot{u}, h, d_x) = -a_{n-1}y^{(n-1)} - \cdots - a_1\dot{y} - a_0 y - g(u) + d_x$, then Eq 5 becomes

$$y^{(n)} = f(t, y^{(n-1)}, \cdots, y, u, \dot{u}, h, d_x) + bu \tag{6}$$

The function $f(.)$ is the total disturbance that contains all nonlinear dynamics of the piezoelectric actuator, unknown complex terms as well as the internal/external disturbances.

The main objective here is to design a suitable control law u so that it is capable of actively rejecting the total disturbance f and achieving a good transient profile. To this end, the ADRC scheme, which consists of an Extended State Observer (ESO) and a feedback controller as shown in Fig 2, is used. The ESO allows the estimation of the total disturbance, while the feedback controller aims to reject the total disturbance while ensuring a good trajectory tracking performance.

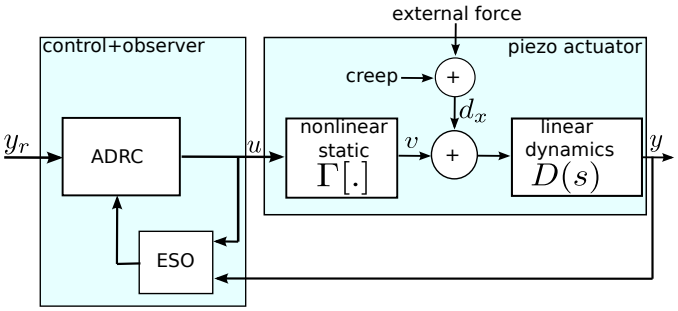

Fig. 2: ADRC control scheme with observer.

The nonlinear representation in Eq 6 can be defined as the following state-space representation:

$$\begin{cases} \dot{x}_1 = x_2 \\ \dot{x}_2 = x_3 \\ \quad\vdots \\ \dot{x}_n = f(t, y^{(n-1)}, \cdots, y, u, \dot{u}, h, d_x) + bu \end{cases} \tag{7}$$

where x_i $(i = 1, 2, ..., n)$ are the system states. Now, let us introduce $x_{n+1} = f$ as an extra-state to form an augmented state-space model from Eq 7:

$$\begin{cases} \dot{x}_1 = x_2 \\ \dot{x}_2 = x_3 \\ \quad\vdots \\ \dot{x}_n = x_{n+1} + bu \\ \dot{x}_{n+1} = p \end{cases} \tag{8}$$

such that f and $p = \dfrac{df(.)}{dt}$ are assumed to be bounded functions. For the purpose of estimating the total disturbance f, an ESO can be constructed using the augmented state-space model as follows [25]:

$$\begin{cases} \dot{\hat{x}}_1 = \hat{x}_2 + g_1(e_1) \\ \dot{\hat{x}}_3 = \hat{x}_3 + g_2(e_1) \\ \quad\vdots \\ \dot{\hat{x}}_n = \hat{x}_{n+1} + g_n(e_1) + bu \\ \dot{\hat{x}}_{n+1} = g_{n+1}(e_1) \end{cases} \tag{9}$$

where $e_1 = x_1 - \hat{x}_1$ is the estimation error. $g_i(.), i = 1, 2, ..., n+1$ are linear or nonlinear functions so that the estimation error converges very closely to zero. For a linear ESO, the functions g_i are selected as $g_i(e_1) = l_i e_i, i = 1, 2, ..., n+1$, where l_i are the ESO gains. In such a linear case, Eq 9 can be rewritten in a compact form as follows:

$$\dot{\hat{x}} = (A - LC)\,\hat{x} + LCx + Bu \tag{10}$$

where

$$x = \begin{bmatrix} x_1 \\ x_2 \\ \vdots \\ x_n \\ x_{n+1} \end{bmatrix};\ \hat{x} = \begin{bmatrix} \hat{x}_1 \\ \hat{x}_2 \\ \vdots \\ \hat{x}_n \\ \hat{x}_{n+1} \end{bmatrix};\ A = \begin{bmatrix} 0 & 1 & 0 & \dots & 0 \\ 0 & 0 & 1 & & 0 \\ \vdots & & \dots & \ddots & 0 \\ 0 & 0 & 0 & \dots & 1 \\ 0 & 0 & 0 & \dots & 0 \end{bmatrix} \tag{11}$$

and

$$B = \begin{bmatrix} 0 \\ \vdots \\ 0 \\ b \\ 0 \end{bmatrix};\ L = \begin{bmatrix} l_1 \\ l_2 \\ \vdots \\ l_n \\ l_{n+1} \end{bmatrix};\ C = \begin{bmatrix} 1 & 0 & 0 & \dots & 0 \end{bmatrix} \tag{12}$$

The ESO gains l_i are often obtained via the bandwidth parameterization approach by placing the eigenvalues of $A - LC$ at a desired position $-w_o$, where w_o is the desired observer bandwidth. Once the ESO is obtained, a state-feedback control law can be constructed from the estimated states to cancel the total disturbance and achieve a satisfactory closed-loop transient profile. The general form of the ADRC law which can be applied to the piezoelectric actuator is expressed as [25]:

$$u = \frac{1}{b}\left(u_0 - \hat{x}_{n+1}\right) \tag{13}$$

u_0 is a new control input to be defined so that the desired closed-loop system performance and stability are met. Under the assumption that the ESO provides a good estimation of the states, the control law above allows the rejection of the total disturbance and results in an n^{th}-order integrator system, i.e. $y^{(n)} \approx u_0$. The control input u_0 is selected as follows:

$$u_0 = k_1(y_r - \hat{x}_1) - k_2\hat{x}_2 - \cdots - k_n\hat{x}_n - \hat{x}_{n+1}$$

such that y_r is the reference input. Equation Eq 13 can be written as

$$u = \frac{k_1}{b}y_r - \frac{1}{b}\begin{bmatrix} k_1 & k_2 & \dots & k_n & 1 \end{bmatrix}\hat{x} \tag{14}$$

k_i are the state feedback gains which can be obtained by applying the bandwidth parameterization approach to place the closed-loop system poles at a desired position $-w_c$ for the purpose of ultimately achieving the desired closed-loop performance specifications.

IV. Experimental Applications

In order to verify the proposed control technique of the previous section, we consider the piezoelectric actuator of stack structure described in Section-II-A.

A. Characterization

First, we characterize the hysteresis phenomenon of the actuator. For that, we apply a sine input voltage of $50[V]$ amplitude to it. Then we record the resulting output displacement $y[\mu m]$. Fig 3-a presents the voltage and the displacement respectively and Fig 3-b presents the input-output map (u, y). This clearly reveals the presence of hysteresis phenomenon of the actuator. Moreover, the hysteresis is strongly asymmetrical. Here, this asymmetry is due to mechanical imperfection (non-symmetry) of the actuator and its surrounding mechanical part. For this experimental response, we extracted the following parameters which will be used for further controller design: $a_0 = 1$, $d = 0.36[\mu m/V]$, $\alpha = 0.08$ and $m = 1$. The hysteresis curve of Fig 3-b was obtained with a sine input of $0.1[Hz]$ frequency. Different experiments shown that when we increase the frequency until several tens of Hertz, the hysteresis curve remains similar to that of Fig 3-b. Beyond $50[Hz]$ the curve starts to be different due to the phase-lag effect. Since the dynamics of the actuator, and thus the phase-lag effect, is accounted by the model $D(s)$, identifying the hysteresis at low frequency is acceptable. Such assumption was also confirmed and used in previous literature [26], [27].

Then, to characterize the dynamics, we apply a step input voltage $u = 50V$ to the actuator. The applied voltage and the output displacement step response are displayed in Fig 4-a and b, blue respectively. It shows that the transient part is characterized by oscillations that are of higher order. Since a pure second order would not be sufficient to approximate this step response, we applied the ARMAX (Auto Regressive Moving Average with eXternal inputs) parametric identification technique with MATLAB to find a precise model [28]. We obtain a 7^{th} order model with 4-zeros as presented in

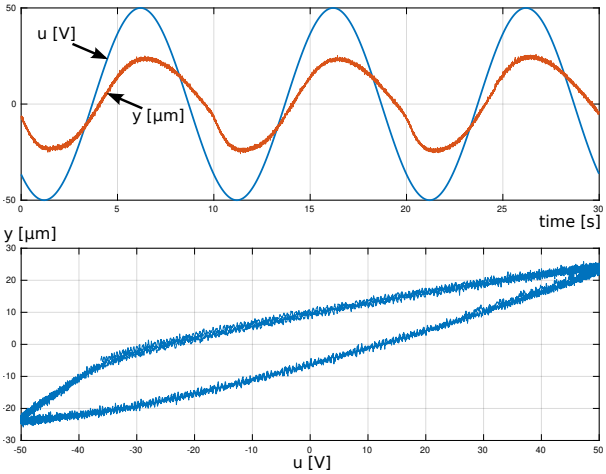

Fig. 3: Hysteresis response of the actuator.

Eq 15. The simulation of the (scaled) model is presented in red dashed-line in Fig 4-b which demonstrates its precision compared to the experimental response. This model will be used for the dynamic part when synthesizing the controller.

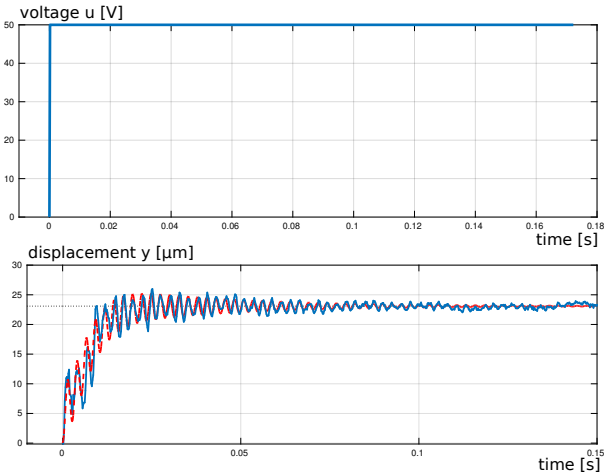

Fig. 4: Step response of the actuator.

$$D(s) = \frac{36\left(s^2+394s+2.4\times10^5\right)\left(s^2+1.7\times10^4 s+9.3\times10^7\right)}{(s+24189)(s^2+494s+6.6\times10^4)(s^2+57s+5.8\times10^6)} \frac{\left(s^2-2041s+2.9\times10^8\right)}{(s^2+96s+2.5\times10^8)} \tag{15}$$

Finally, to characterize the creep phenomenon, we still apply a step voltage $u = 50[V]$. Contrary to the dynamics characterization previously, we observe the step response for a much longer time $(600s)$. Fig 5 displays the observed step response. In this, the creep is the slow drift that appears after the transient part $(0.18s)$ finishes. Such phenomenon definitely decreases the precision of a manipulation task if not controlled.

B. Feedback control

The controller and observer proposed in section-III have been implemented using identified parameters from section-

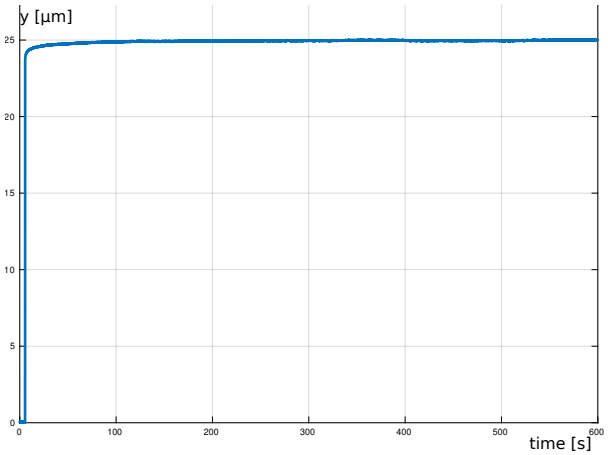

Fig. 5: Creep response of the actuator.

IV and the implementation scheme in Fig 2.

First, in order to check the suppression of the hysteresis, we applied a sine reference input y_r of $20[\mu m]$ amplitude. Several frequencies have been used. Fig 7 displays the result when using a frequency of $10[Hz]$ which demonstrates the complete suppression of the hysteresis. Above certain frequency (around $50[Hz]$), the input-output map curve starts exhibiting a phase-lag effect. Since the studied hysteresis is a low-frequency phenomenon as per the Hammerstein approximation (see Fig 1-c) and the phase-lag is purely related to the dynamics of the closed-loop, we can consequently confirm that the hysteresis was removed by the controller.

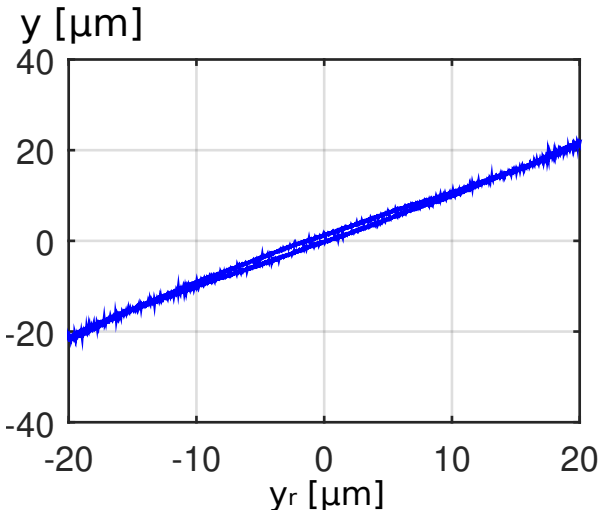

Fig. 6: Feedback input-output response to a sine reference.

Finally, we apply a step reference input of $y_r = 20[\mu m]$ amplitude to the closed-loop. Fig 7 displays the result. It reveals that we reduced the 5% settling time from in excess of $50[ms]$ (calculated from the open-loop response in Fig 4-b) to $10[ms]$ (calculated from Fig 7) additionally to the suppression of the vibrations and of the overshoot. Moreover, the final value of the closed-loop step response shows that there is no static error and thus the accuracy is high.

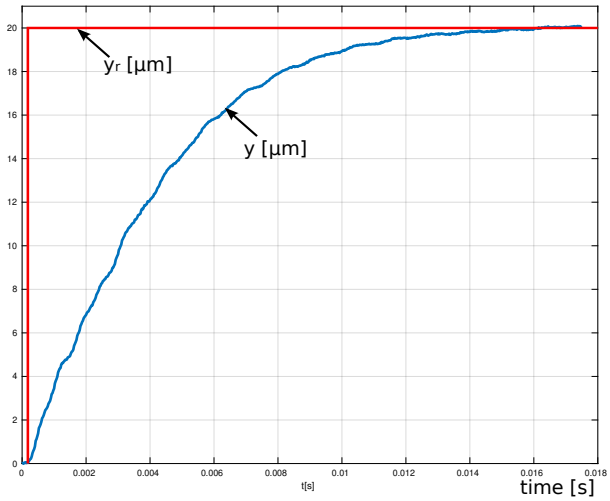

Fig. 7: Feedback step response to a reference $y_r = 20\mu m$.

C. Discussions

The above experiments demonstrate the efficiency of the feedback controller combined with the extended state observer (ESO). The observer was used to estimate the state and the additional state (disturbance) of the system. To this, the output y was still measured using an external sensor. In this work, we specifically used an inductive sensor (ECL202 from *Lion Precision* company) tuned to have $1[kHz]$ bandwidth and some nanometers resolution. Despite the good performances, such sensor is bulky and will not be appropriate for the entire robotic hand. Integrated sensors will therefore be needed. Several avenues are being evaluated and will be studied as perspective of this work. The first consists in implementing classical strain gage to each of the three actuators. Their main advantage is the high integration thanks to their small size. Moreover some commercialized piezoelectric actuators are readily equipped with strain gage sensors. In counterpart, these sensors are very fragile and in some cases could have limited range of measurable displacement. Another avenue of integrated measurement consists in using the piezoelectric actuator as its proper sensor. Called self-sensing, the princile consists in combining the direct piezoelectric effect (sensing) with the converse effect (actuation) thanks to a judicious electronic circuit connected to the piezoelectric actuator. Piezoelectric self-sensing was widely used for vibration damping [29], [30] as it is efficient at high frequency and loses performances at low frequency or constant signals. These last years were witnessed by its adaptation to work at low frequency and constant signals [31], [32]. Recently, an appropriate observer combined with the electronic circuit of the piezoelectric self-sensing allowed to work at both high and low frequency and to estimate acceleration, velocity and position at the same time [33]. This latter self-sensing approach has a very interesting feature that could be combined with the ADRC and ESO technique developed in this paper. Perspective works will therefore be in this direction.

V. Conclusion

This paper presented the modeling and the control of a piezoelectric actuator devoted to actuate a robotic hand. The actuator was characterized by strong nonlinearities (hysteresis and creep) as well as oscillations in its dynamics. Furthermore, the actuator was aimed to be in contact with manipulated objects and thus subjected to external force disturbance. We proposed to model the hysteresis, assumed to be asymmetrical, with the Bouc-Wen modeling approach and rassembled the creep and the force as one single disturbance. Moreover, we considered a high order dynamics to account for any oscillations. Afterwards, we proposed an active disturbance rejection control (ADRC) law to control the actuator by accounting for the above properties. Since the ADRC needed a real-time knowledge of the disturbance which was unknown for our case, we proposed to consider this latter as an additional state and thus we designed an extended state observer (ESO) for its estimation. The proposed combined ADRC ESO control technique was tested and its performances were demonstrated. Because the ADRC ESO still needed real-time knowledge of the output displacement, we utilized an external sensor for its measurement. Such external sensor is not appropriate for future application with the robotic hand. Perspective work will consist therefore in studying embeddable measurement technique such as the piezoelectric self-sensing.

Acknowledgments

This work is partially supported by the French CPER ECOSYSPRO project.

References

[1] S. Kon et al., 'Design and fabrication of a piezoelectric instrumented suspension for hard disk drives', Proceedings of SPIE, March 2006.

[2] L. S. Mattos et al., 'µRALP and beyond: Micro-technologies and systems for robot-assisted endoscopic laser microsurgery', Frontiers in Robotics and AI, section Biomedical Robotics, https://doi.org/10.3389/frobt.2021.664655, September 2021.

[3] D. Arun et al., 'Piezosurgery in dentistry', Journal of Oral Research and Review 8(1):27, January 2016.

[4] F. J. Salvador et al., 'Complete modelling of a piezo actuator last-generation injector for diesel injection systems', International Journal of Engine Research 15(1):3-19, January 2012.

[5] G. Binnig et al., 'Atomic Force Microscope', Physical Review Letters, 56(9): 930–933, March 1986.

[6] G. Flores and M. Rakotondrabe, 'Robust nonlinear control for a piezoelectric actuator in a robotic hand using only position measurements', IEEE Control Systems Letters, Vol.6, pp.872-877, 2022.

[7] M. Rakotondrabe and A. Ivan, 'Development and dynamic modeling of a new hybrid thermo-piezoelectric micro-actuator', IEEE Transactions on Robotics, Vol.26(6), pp.1077-1085, Dec 2010.

[8] S. Khadraoui et al., ' Optimal design of piezoelectric cantilevered actuators with guaranteed performances by using interval techniques', IEEE/ASME Transactions on Mechatronics, Vol.19(5), pp.1660-1668, Oct 2014.

[9] A. Homayouni at al., '2D Topology Optimization MATLAB Codes for Piezoelectric Actuators and Energy Harvesters', Structural and Multidisciplinary Optimization, 106880, Vol.1452020, Oct 2020.

[10] M. Rakotondrabe, 'Modeling and Compensation of Multivariable Creep in multi-DOF Piezoelectric Actuators', IEEE Int. Conference on Robotics and Automation, pp.4577-4581, St Paul Minnesota USA, 2012.

[11] M. Rakotondrabe, 'Multivariable classical Prandtl-Ishlinskii hysteresis modeling and compensation and sensorless control of a nonlinear 2-dof piezoactuator', Nonlinear Dynamics, DOI: 10.1007/s11071-017-3466-5, 2017.

[12] R. Oubellil et al., 'Experimental model inverse-based hysteresis compensation on a piezoelectric actuator', IEEE Int Conf on System Theory, Control and Computing, pp.186-191, Cheile Gradistei, Romania, Oct 2015.

[13] D. Croft and S. Devasia, 'Vibration compensation for high speed scanning tunneling microscopy', Review of Scientific Instruments, 70(12), 1999.

[14] Y. Al Hamidi et al., 'Multi-Mode Vibration Suppression in a multi-DOF Piezoelectric Tube Actuator by extending the Zero Placement Input Shaping Technique', MDPI Actuators, 5(2), 13, April, 2016.

[15] D. Croft et al., 'Creep, hysteresis, and vibration compensation for piezoactuators: atomic force microscopy application', Journal Dynamical Systems, Measurement, Control 123(1), 35-43, 2001.

[16] D. Habineza et al., 'Multivariable compensation of hysteresis, creep, badly damped vibration and cross-couplings in multi-axes piezoelectric actuators', IEEE Trans on Automation Science and Engineering, 15(4), pp.1639-1653, Oct 2018.

[17] A. Youssef, 'Optimized PID tracking controller for piezoelectric hysteretic actuator model', World Journal of Modelling and Simulation, 9(3), pp.223-234, 2013.

[18] J. Ling et al., 'A Robust Resonant Controller for High-speed Scanning of Nanopositioners: Design and Implementation', IEEE Trans on Control Systems Technology, DOI.10.1109/TCST.2019.2899566, 2019.

[19] Y-T. Liu and K-M. Chang, 'Model reference adaptive control for a piezo-positioning system', Precision Engineering 34(1):62-69, Jan 2010.

[20] H. Ladjal et al., 'H Infinity robustification control of existing piezoelectric-stack actuated nanomanipulators', IEEE Int Conf on Robotics and Automation, Kobe Japan, May 2009.

[21] M. Rakotondrabe, 'Performances inclusion for stable interval systems', American Control Conference, 4367-4372, 2011.

[22] S Khadraoui et al., 'Combining H-inf approach and interval tools to design a low order and robust controller for systems with parametric uncertainties: application to piezoelectric actuators', International Journal of control, 85(3), 251-259, 2012.

[23] J.A. Escareno et al., 'Backstepping-based robust-adaptive control of a nonlinear 2-DOF piezoactuator' Control Engineering Practice, 41, 57-71, 2015.

[24] G. Flores et al., 'Model predictive control based on the generalized Bouc-Wen model for piezoelectric actuators in robotic hand with only position measurements', IEEE Control Systems Letters, 6, pp.2186-2191, 2022.

[25] B-Z. Guo and Z-L. Zhao, 'Active Disturbance Rejection Control for Nonlinear Systems: An Introduction', John Wiley Sons, ISBN:9781119239925, 2016.

[26] K. K. Leang and S. Devasia, 'Feedback-linearized inverse feedforward for creep, hysteresis, and vibration compensation in AFM piezoactuators', IEEE Trans on Control Systems Technology, 15(5), 927-935, 2007.

[27] O. Aljanaideh et al., 'Experimental comparison of rate-dependent hysteresis models in characterizing and compensating hysteresis of piezoelectric tube actuators', Physica B: Condensed Matter, 486, 64-68, 2016.

[28] L. Ljung, 'System identification toolbox', The matlab user's guide, 2011.

[29] J.J. Dosch et al., 'A Self-Sensing Piezo- electric Actuator for Collocated Control', Journal of Intell. Mater. Syst. and Struct., 3, pp. 166-185, 1992.

[30] M..G. Ruppert and R. Moheimani, 'High-bandwidth multimode self-sensing in bimodal atomicforce microscopy', Journal of Nanotechnology, vol.7, 284-295, Feb 2016.

[31] I.A. Ivan and al., 'Quasi-static displacement self-sensing method for cantilevered piezoelectric actuators', Review of Scientific Instruments (RSI), Vol.80(6), 065102, June 2009.

[32] A. A. Ivan et al., 'Quasi-static displacement self-sensing measurement for a 2-DOF piezoelectric cantilevered actuator', IEEE Transactions on Industrial Electronics, DOI.10.1109/TIE.2017.2677304, 2017.

[33] M. Rakotondrabe, 'Combining self-sensing with an Unkown-Input-Observer to estimate the displacement, the force and the state in piezoelectric cantilevered actuator', American Control Conference, pp.4523-4530, Washington DC USA, June 2013.